



Published in final edited form as:

Cancer Immunol Res. 2015 August ; 3(8): 956–967. doi:10.1158/2326-6066.CIR-15-0015.

Melanoma induces, and adenosine suppresses, CXCR3-cognate chemokine production and T-cell infiltration of lungs bearing metastatic-like disease

Eleanor Clancy-Thompson^{1,2,5}, Thomas J. Perekslis^{1,2}, Walburga Croteau³, Matthew P. Alexander^{1,2}, Tamer B. Chabanet^{1,2}, Mary Jo Turk^{1,2}, Yina H. Huang^{1,3}, and David W. Mullins^{1,2,4}

¹Department of Microbiology and Immunology, Geisel School of Medicine at Dartmouth, Lebanon, NH 03756

²Norris Cotton Cancer Center, Geisel School of Medicine at Dartmouth, Lebanon, NH 03756

³Department of Pathology, Geisel School of Medicine at Dartmouth, Lebanon, NH 03756

Abstract

Despite immunogenicity, melanoma-specific vaccines have demonstrated minimal clinical efficacy in patients with established disease but enhance survival when administered in the adjuvant setting. Therefore, we hypothesized that organs bearing metastatic-like melanoma may differentially produce T-cell chemotactic proteins over the course of tumor development. Using an established model of metastatic-like melanoma in lungs, we assessed the production of specific cytokines and chemokines over a time-course of tumor growth, and we correlated chemokine production with chemokine receptor-specific T-cell infiltration. We observed that the interferon (IFN)-inducible CXCR3-cognate chemokines (CXCL9 and CXCL10) were significantly increased in lungs bearing minimal metastatic lesions, but chemokine production was at or below basal levels in lungs with substantial disease. Chemokine production correlated with infiltration of the organ compartment by adoptively transferred CD8⁺ tumor antigen-specific T cells in a CXCR3- and host IFN γ -dependent manner. Adenosine signaling in the tumor microenvironment suppressed chemokine production and T-cell infiltration in the advanced metastatic lesions, and this suppression could be partially reversed by administration of the adenosine receptor antagonist aminophylline. Collectively, our data demonstrate that CXCR3-cognate ligand expression is required for efficient T cell access of tumor-infiltrated lungs, and these ligands are expressed in a temporally restricted pattern that is governed, in part, by adenosine. Therefore, pharmacologic modulation of adenosine activity in the tumor microenvironment could impart therapeutic efficacy to immunogenic but clinically ineffective vaccine platforms.

⁴Corresponding author's Address: Norris Cotton Cancer Center, Geisel School of Medicine at Dartmouth, 1 Medical Center Drive, HB7937, Lebanon, NH 03756. Voice: 603.653.9922. FAX: 603.653.9952. david.w.mullins@dartmouth.edu.

⁵Current Address: Dana-Farber Cancer Institute, 450 Brookline Avenue, Boston, MA 02215.

Disclosures: Dr. Mullins is a scientific advisor to Qu Biologics, Vancouver BC Canada; Qu Biologics has provided contract funding for specific research that is unrelated to the current manuscript.

Keywords

Adenosine; A_{2A}R; CXCR3; CXCL9; CXCL10; CD8 T cells; melanoma

Introduction

Active vaccination has proven immunogenic (1), increasing the number of circulating tumor antigen-specific CD8⁺ effector or memory T cells. However, therapeutic vaccination imparts minimal clinical efficacy against active disease (2), even though *ex vivo* analyses demonstrate that vaccine-induced cytotoxic T lymphocytes lyse tumor targets *in vitro* (3). The failure of vaccines in the context of active disease may be ascribed to tumor-induced local immune suppression, myeloid-derived suppressor cells (MDSC) or regulatory T-cell (Treg) activity, or tumor immune editing to evade T-cell recognition (4). However, T cell access of tumors is associated with improved prognosis in primary (5) and metastatic (6) melanomas, yet multiple studies have demonstrated that effector T-cell infiltration of primary or metastatic melanomas is variable and often absent. Thus, the efficacy of vaccination likely relies upon efficient infiltration of tumors by treatment-induced antigen-specific T cells.

Circulating effector T cells access peripheral tissues, including tumors and tumor-infiltrated organs, through the engagement of integrins with their ligands on the vascular endothelium; firm adhesion and extravasation of T cells requires high-affinity integrin binding, which is activated by chemokine receptor (CCR) in response to specific ligands (chemokines). Recent studies have highlighted the clinical importance of chemokine expression for T-cell infiltration into the tumor microenvironment (TME) (7). Likewise, expression of CXCR3-cognate chemokines (CXCL9, CXCL10, and CXCL11) is correlated with T-cell infiltration status in metastatic melanoma (8). Previously, we demonstrated that melanoma cells from lymph node metastases are capable of producing CXCR3-cognate chemokines following stimulation with interferon (IFN)- α or IFN γ (9). Furthermore, the presence of tumor-specific CD8 cells expressing CXCR3 correlated with the duration of survival (10). Collectively, these observations suggest an important role for the CXCR3 chemotactic axis for the temporal and spatial targeting of circulating T effector cells to compartments with melanoma metastases.

While vaccination has shown minimal efficacy for treatment of advanced disease, adjuvant-setting vaccination has prolonged disease-free survival (11), suggesting that newly-forming metastatic lesions may be receptive to T-cell infiltration, and by extension, replete with chemokines; in contrast, more advanced and established tumors may lack T-cell infiltration as a consequence of suppressed chemokine production. To date, no study has evaluated the possibility of differential chemokine production and T-cell infiltration over the course of tumor growth.

Using an established murine model of metastatic-like melanoma in the lungs, we demonstrate differential regulation of CXCR3-cognate chemokine and infiltration by CXCR3⁺CD8⁺ T cells in early versus advanced-stage tumors. Importantly, T-cell infiltration of advanced tumors can be partially restored through blockade of adenosine receptor

signaling. Thus, we demonstrate a deficit in immune therapy of cancer and a potential means to enhance the antitumor efficacy of vaccine or adoptive T cell-mediated therapy of established metastatic disease.

Methods

Tumor models

Metastatic-like tumors were established in C57BL/6 mice (Jackson Laboratory strain 00664), Rag^{-/-} (Jackson Laboratory strain 002216), or IFN γ ^{-/-} (Jackson Laboratory strain 002287), as indicated, by intravenous injection of 3×10^5 B16-F10 (B16) melanoma cells. B16 cells were obtained from ATCC (CRL-6475), and tumors were established from cryopreserved stocks that had been passaged less than two times. Tumor development was observed in 100% of injected mice.

Inducible melanomas were established by intradermal injection of 4-hydroxy-tamoxifen (10 μ l of a 20 μ M solution in DMSO) in Tyr::CreER^{+/-}; Braf^{CA/+}; Pten^{lox/lox} mice (12) that had been backcrossed onto a B6 background, as described (13).

For all studies, animals were maintained in pathogen-free facilities at the Geisel School of Medicine, and all procedures were approved by the Dartmouth College *Institutional Animal Care and Use Committee*.

Cytokine and chemokine production analyses

Protein from perfused lungs was isolated using Total Protein Extraction Reagent (Thermo Scientific) and cOmplete protease inhibitor (Roche cOmplete). Mouse CXCL9, CXCL10, and IFN γ ELISA (DuoSets) were obtained from R&D Systems and performed according to the manufacturer's protocol.

Gene expression analyses

Total RNA from cultured B16 melanoma cells, perfused lungs, or Braf/Pten tumors was isolated (Qiagen RNeasy kit) then translated into cDNA using a High Capacity RNA-to-cDNA kit (Applied Biosystems). Specific gene expression was quantified by qPCR using master mix and pre-validated gene-specific primers (Life Technologies) and a StepOne Plus instrument (Applied Biosystems).

Lung sections and immunohistochemistry

Mice were perfused with 4% paraformaldehyde (PFA, Sigma-Aldrich) prior to lung dissection. Lungs were sequentially incubated for 1 hour at 4°C in i) 4% PFA, ii) 30% sucrose in PBS, and iii) 15% sucrose, 50% OCT (Tissue Tek, Sakura) in PBS followed by embedding in OCT. 10 μ m sections were performed with a cryostat, fixed in cold acetone, rehydrated in PBS and blocked in 5% BSA in PBS. Sections were stained overnight with primary antibodies against CXCL9, CXCL10 (rabbit, Bioss) and TA99 (ATCC clone HB-8704), followed by Alexa594- and Alexa647-conjugated secondary antibodies against mouse and rabbit IgG in 1% normal goat serum (Jackson ImmunoResearch and Life Technologies), for 1 hour at room temperature. Microscopy was performed on a Zeiss AX10

fluorescence microscope fitted with a CoolSnap HQ2 mono14-bit camera, using a 20X Apo objective. Images were taken with ZEN Pro 2012 (Zeiss) software and processed with Fiji image processing software.

Reagents

Antibodies specific for murine CD183 (CXCR3, clone CXCR3 173), CXCL9 (clone MIG 2F5.5), IFN γ (clone XMG1.2), CD4 (clone RM4-5), CD8 α (clone 5H10-1), CD45 (clone 30-F11), CD11c (clone N418), Ly6G (clone 1A8), CD335 ([NKp46], clone 29A1.4), CD90.1 (Thy1.1, clone OX-7), CD31 (clone 390), and CD16/32 (clone 93) were obtained from BioLegend. Anti-Adenosine A_{2a} receptor (ADORA2A) (clone 7F6-G5-A2) was obtained from Novus Biologicals.

Adoptive transfer model

Tumors were allowed to establish for 3, 11, or 18 days before adoptive transfer of T cells. T cells for adoptive transfer were collected from spleens of T-cell receptor (TCR) transgenic donor mice. To facilitate tracking of transferred cells, specific TCR mice were crossed onto a Thy1.1 x Rag^{-/-} background (Jackson Laboratory strains 000406 and 002216, respectively). To ensure tumor-antigen specificity, T cells specific for an endogenous melanocyte/melanoma antigen (gp100) were obtained from Pmel x Thy1.1 x Rag^{-/-} mice (crossed from Pmel TCR mice, Jackson Laboratory strain 005023; henceforth termed Pmel mice); these mice were then crossed onto a CXCR3-deficient background and henceforth termed Pmel/CXCR3^{-/-} mice.

Prior to transfer, TCR transgenic CD8 T cells were enriched using a MACs negative selection magnetic kit (Miltenyi), then activated by culture (37°C/5% CO₂ for 24 hours) with anti-CD3 and anti-CD28 Dynabeads (Life Technologies) at a 1:1 ratio. For adoptive transfer studies, 1×10⁶ *in vitro*-activated CD8⁺ Pmel or Pmel/CXCR3^{-/-} cells were intravenously injected into mice at various stages of tumor growth, as indicated, then recovered and enumerated 1 hr later (14).

To assess T-cell infiltration of tumor-bearing lungs, the lungs were perfused with 1mL 1X PBS and homogenized to single-cell suspensions and enriched for lymphocytes using a gentleMACS tissue dissociator and lung dissociation kit (Miltenyi). Magnitude of T-cell infiltration was assessed by multi-color flow cytometry (MACSQuant, Miltenyi). Monoclonal antibodies against CD8, CD45, CXCR3, and Thy1.1 (Biolegend) were used to track adoptively transferred T cells, and viability was confirmed with violet viability dye (Life Technologies).

Flow cytometric staining and analyses

For surface staining, cells were suspended in FACS buffer (1% BSA in PBS) and incubated with purified antibodies for 30 min at 4°C, then washed 3x in FACS buffer and fixed in 0.5% paraformaldehyde. For intracellular staining, cells were stained for surface markers and fixed with a 1:4 dilution of Fixation Buffer (Biolegend) in PBS for 20 minutes; washed twice with a 1:10 dilution of Permeabilization Buffer (Biolegend) in PBS (Perm Buffer); incubated in Perm Buffer for 20 minutes; stained for CXCL9 or IFN γ in Perm Buffer for 30

min; and washed twice with FACS buffer. All data were acquired with a Miltenyi MacsQuant cytometer and analyzed with FlowJo (TreeStar) software.

In vitro migration studies

To assess the migration potential of CD8⁺ T cells from Pmel and Pmel/CXCR3^{-/-} mice, magnetically enriched CD8 T cells (Miltenyi) were activated, as described above, and plated at 5×10^4 cells into transwell assay plates with 5 μ M membranes (Costar). Chemokines (CXCL10 or CCL5, RND Systems) were added to the bottom wells, and chemokine receptor-specific blocking antibody (anti-CXCR3, BioLegend CXCR-173) added to the top wells, as indicated. After 3h incubation at 37°C, migrated cells were enumerated using an automated cell counter (BioRad TC10).

Aminophylline treatment

To assess the role of adenosine-mediated signaling on cytokine and chemokine expression and production in the TME, tumor-bearing mice were treated with the nonspecific adenosine receptor antagonist aminophylline (theophylline ethylenediamine, Sigma Aldrich) by I.P. injection of 50 μ g/mL of drug every 3 days for 18 days, as described (15).

In vitro tumor studies

B16 melanomas were plated at 1×10^5 cells per well in 24-well tissue culture plates (Corning) at 37°C/5% CO₂. After 24 hours, the supernatant was replaced and amended with IFN γ (0, 500, 2,500, or 5,000 pg; BioLegend), adenosine (ADO) (0, 500, or 1,000 μ M, Tocris), or the adenosine A2 receptor-specific inhibitor ZM241,385 (ZM; 0 μ M, 10 μ M, RND Systems). After 24 hours at 37°C/5% CO₂, the supernatant was collected and CXCL10 protein production measured by ELISA.

Results

Differential CXCR3-cognate chemokine production over the course of tumor growth

We hypothesized that tumor engraftment may transiently induce, and then suppress, CXCR3-cognate chemokine production in the lungs. To explore this possibility, we used a well-characterized model of metastatic-like melanoma and evaluated CXCL9 and CXCL10 production at various time points following injection and establishment of tumors.

In the unperturbed lung compartment, we detected CXCL9 and CXCL10 protein (Figure 1A–B), consistent with high level of *cxc19* and *cxc110* expression in CXCR3-competent C57BL/6 mice (16). Three days after injection of B16 melanoma, we detected significant increases in CXCL9 (Figure 1A, $p < 0.0002$) and CXCL10 (Figure 1B, $p < 0.05$) proteins, relative to lungs without tumor. At this time point, there was minimal detectable gp100 (melanoma-specific gene) in the lungs (Supplemental Figure 1A), suggesting minimal residual tumor burden. By eleven days post tumor-injection, CXCL9 and CXCL10 production was significantly ($p < 0.001$ for both proteins) lower than that observed at day 3. After eighteen days of tumor growth, when tumor burden was substantial, chemokine levels were comparable (CXCL9, $p = 0.06$) or lower (CXCL10, $p = 0.0003$) than basal levels. From day 3 to day 18, CXCL9 and CXCL10 were significantly ($p < 0.0001$ and $R^2 = 0.7401$, and

$p=0.0002$ and $R^2=0.6879$, respectively) inversely correlated with gp100 signal (Supplemental Figure 1 B–C). *Cxcl9* and *cxcl10* expression by qPCR corresponded with observed protein production (not shown). Thus, melanoma transiently induces the expression and production of CXCL9 and CXCL10 in lungs bearing metastatic-like tumors.

The observed production of CXCL9 and CXCL10 at three days post-tumor injection is not likely the consequence of tumor cell injection-induced transient ischemia. We observed no change in CXCL9 and CXCL10 production at day one post-injection, but significant increases in chemokine production by day 2 (Supplemental Figure 2A–B). In contrast, Medoff and colleagues reported a rapid and short-lived production of CXCL10 in an injury-induced ischemia model (17). These data discount the role of transient ischemia in chemokine production in our model and suggest that chemokine production in tumor-burdened lung is a consequence of tumor engraftment.

To assess whether spontaneous tumors also suppress CXCR3-cognate chemokine production as a function of growth, we assessed the expression of *cxcl9* and *cxcl10* in early (~5mm², day 25) and late (~25mm², day 40) Braf/Pten tumors using an inducible model (13). The timing of assessment is offset, relative to a transplantable model, as inducible tumors require ~2 weeks to become palpable and assessable (13). Consistent with our observations in the transplantable model, we observed higher levels of chemokine gene expression in early tumors, as compared with that in late tumors (Supplemental Figure 3). Likewise, we have observed a similar temporal regulation of CXCL9 and CXCL10 in subcutaneously implanted B16 melanoma (data not shown). These data suggest that tumor-induced CXCR3-cognate chemokine production, and subsequent suppression, may occur in clinically relevant cancers.

Our primary studies evaluated chemokine production in the tumor-bearing lung compartment, rather than in isolated tumors. Thus, our chemokine data from the lung studies represent the total tumor-bearing organ. To more precisely define the source of chemokine in this model, we assessed CXCL9 and CXCL10 by immunohistochemical staining of lungs bearing day 3 tumors (Figure 2A–C), corresponding to peak chemokine production. Specific staining for CXCL9 (Figure 2B, green) and CXCL10 (Figure 2C, green) was localized in proximity of melanoma-specific staining (red), including co-localization, suggesting melanoma is a source of chemokine. Melanoma production of chemokine is consistent with prior observations in patient-derived cell lines (9) and tumors (8), and we observed that B16 melanoma produces CXCL10 in response to IFN γ stimulation *in vitro* (Supplemental Figure 4A). In keeping with this observation, CD45⁻CD31⁻FSC^{hi}SSC^{hi} cells (putative tumor cells) from early (day 3) lungs produced CXCL9, whereas CXCL9 was mostly ablated in this cell population by day 18, suggesting that melanoma may be a major source of chemokine in this model (Supplemental Figure 4B). Chemokine production was also observed in non-tumor cells (Supplemental Figure 5). CD4 T cells and neutrophils are the major non-tumor CXCL9-producing cell populations in tumor-bearing lungs (Figure 2D and Supplemental Figure 5A). Surprisingly, only a small proportion of CD45⁻CD31⁺ endothelial cells were positive for CXCL9 (Figure 2D). Thus, tumor cells and immune cells are likely to be the major contributors to CXCR3-cognate chemokine in the lung during early metastatic tumor growth.

Differential interferon production over the course of tumor growth

Interferons are major inducers of CXCL9 and CXCL10 expression and production (18). Therefore, we evaluated IFN γ (type II) and IFN α (type I) in our murine tumor model of metastatic-like melanoma in the lungs. IFN γ production in the lungs was significantly ($p < 0.005$) enhanced at day 3 post tumor induction, relative to mice with no tumor. Importantly, IFN γ production was significantly diminished by day 18, relative to day 3 levels ($p < 0.0005$) or basal levels ($p < 0.01$) (Figure 3A). Similarly, *Ifna* expression was significantly enhanced on day 3 ($p < 0.001$) versus mice with no tumor, and significantly reduced from day 3 to day 18 ($p < 0.0001$) (Figure 3B). The induction of IFN expression is not a consequence of transient tumor injection-induced ischemia, as no increase in IFN production or expression was observed at day 1 post-tumor injection (data not shown). Comparable temporal regulation of IFN γ expression was also observed in the Braf/Pten inducible tumor model (data not shown). These data demonstrate that engrafting melanomas induce IFN γ and IFN α , and these cytokines likely induce CXCL9 and CXCL10 production in the tumor-bearing organ.

Melanoma is an unlikely source of interferon production, and we have not detected IFN γ or IFN α protein or *Ifn γ* or *Ifna* gene expression in cultured B16 or human melanoma cell lines, even in response to stimulation with exogenous TNF α (data not shown). We assessed IFN γ production in non-tumor cells by intracellular flow cytometry (9), in tandem with specific lineage markers. CD4 T cells are the predominant non-tumor population of IFN γ -producing cells in tumor-bearing lungs (Figure 3C and Supplemental Figure 5B); as observed for chemokine, only a small number of CD45⁻CD31⁺ endothelial cells were positive for IFN γ .

Differential T-cell infiltration over the course of tumor growth corresponds with production of CXCR3 ligands

We previously associated survival with the presence of circulating CXCR3⁺CD8⁺ tumor-specific T cells (10), and the presence of infiltrating CD8 T cells in human melanoma metastases has been associated with a defined set of chemokines, including CXCL9 and CXCL10 (8). Therefore, we hypothesized that T-cell infiltration of melanoma-engrafted lungs may require CXCR3-cognate chemokines. To assess this possibility, we transferred *in vitro*-activated, tumor-specific (Pmel) CD8⁺ T cells into unchallenged Rag^{-/-} mice or tumor-challenged Rag^{-/-} mice at 3, 11, or 18 days after tumor injection, then assessed T-cell infiltration of lungs one hour after transfer (14). The majority of activated Pmel cells express CXCR3 (Supplemental Figure 6).

In agreement with our hypothesis, Pmel CD8⁺ T cells traffic more efficiently to metastatic tumor-involved lungs in the early phase of growth (day 3), versus lungs bearing more established (day 18) tumors ($p < 0.0001$) (Figure 4A). T-cell infiltration at day 18 was lower ($p < 0.001$) than basal levels of infiltration in tumor-free mice. Results of these studies were similar in B6 (Rag^{WT}) tumor hosts (data not shown). These data demonstrate that T-cell infiltration of metastatic tumor-bearing lungs correlates with melanoma-induced production of IFN γ and CXCR3-cognate chemokines, and that T cell access to the organ compartment becomes compromised over the course of tumor growth.

To confirm a requirement for IFN γ in the trafficking of transferred Pmel T cells to metastatic melanomas, we used IFN $\gamma^{-/-}$ mice as tumor hosts. After transfer of Pmel CD8 $^{+}$ T cells into mice with day 3 inflammatory lung metastases, the number of lung-infiltrating T cells was significantly decreased in IFN $\gamma^{-/-}$ mice, as compared with comparable tumor-bearing Rag $^{-/-}$ hosts ($p < 0.001$, Figure 4B) or B6 hosts ($p < 0.05$, Supplemental Figure 7A). Interestingly, in the IFN $\gamma^{-/-}$ host, the number of transferred T cells in the spleen was significantly greater than that in tumor-bearing lung ($p = 0.01$) (Supplemental Figure 7B), consistent with the lack of chemoattraction of T cells into inflamed peripheral organs in these mice. Therefore, T-cell infiltration of metastatic tumor-bearing lungs requires host expression of IFN γ , likely as the inducer of CXCL9 and CXCL10.

CXCR3-expressing CD8 T cells are preferentially recruited to tumor-bearing lung during early phases of tumor growth

The observed correlation between CXCL9 and CXCL10 production and T-cell infiltration in lungs suggest that CXCR3 may play a significant role in CD8 T cell access of tumor-bearing lungs. To assess the role of T cell-expressed CXCR3, we compared the infiltration of *in vitro*-activated CD8 $^{+}$ Pmel and Pmel/CXCR3 $^{-/-}$ T cells in Rag $^{-/-}$ hosts bearing day 3 lung metastases. Tumor antigen-specific CXCR3 $^{+}$ CD8 $^{+}$ T cells infiltrated tumor-bearing lungs to a greater extent than cells lacking CXCR3 ($p < 0.0005$) (Figure 4C–D), even though adoptively transferred CXCR3 $^{+}$ and CXCR3 $^{-/-}$ cells were equivalently represented in the spleen (Supplemental Figure 7C).

Over the course of tumor growth, infiltration by CXCR3 $^{+}$ Pmel T cells was significantly and consistently greater than Pmel/CXCR3 $^{-/-}$ cells (Figure 4E); CXCR3 $^{+}$ T-cell infiltration coordinated with the level of observed CXCR3 ligands in the organ compartment, whereas infiltration by Pmel/CXCR3 $^{-/-}$ T cells did not significantly change over the course of tumor growth. Therefore, CXCR3 is critical for T-cell infiltration during early phases of tumor development, but is insufficient to facilitate T cell access of organs with significant tumor load and a dearth of CXCR3-cognate chemokines.

Consistent with data from Thapa and colleagues (19), we observed that Pmel/CXCR3 $^{-/-}$ CD8 T cells were less capable of lysing target cells (Supplemental Figure 8A), indicating reduced effector function. However, pharmacologic activation induced comparable proportions of IFN γ^{+} cells from Pmel or Pmel/CXCR3 $^{-/-}$ mice (Supplemental Figure 8B), and ablation of CXCR3 did not diminish the capacity of the CD8 cells to migrate in response to CCR5-specific chemokine (CCL5, Supplemental Figure 8C). Thus, while loss of CXCR3 may negatively impact cell-mediated effector function, our short-term studies are designed to assess the impact of CXCR3 on T-cell infiltration (14), and the uncoupling of effector function and migratory activity (19,20) validates our model for this purpose.

Adenosine signaling suppresses interferon and CXCR3-cognate chemokine production in melanoma

Our data suggest that IFN and CXCR3-cognate chemokine may be suppressed in lungs bearing advanced melanomas. However, the mechanism of suppression is undefined. Because free adenosine accumulates in hypoxic tumor microenvironments (21) such as the

advanced metastatic lesions in our model system, and adenosine signaling via A₂ receptors (A₂R) suppresses IFN-inducible CXCL9 and CXCL10 production in immune cells (22), we assessed the possibility that adenosine signaling may suppress cytokine and chemokine production in metastasis-bearing lungs. Administration of the clinically available non-selective adenosine receptor antagonist aminophylline (23) to tumor-bearing mice significantly increased CXCL9 (p<0.001), CXCL10 (p<0.0005), and IFN γ (p<0.01) production in lungs bearing established, day 18 melanoma metastases (Figure 5A–C). Aminophylline treatment had no effect on CXCL9, CXCL10, or IFN γ production in tumor-free lungs (Supplemental Figure 9 and data not shown).

As aminophylline treatment partially restored chemokine production in lungs with advanced melanoma, we assessed whether treatment with this adenosine receptor antagonist could enhance T-cell infiltration in lungs with advanced melanoma that suppresses CXCR3-cognate chemokine production. Using the adoptive transfer model described above, we assessed T-cell infiltration of lungs bearing day 18 melanoma following treatment with aminophylline or vehicle (PBS). T-cell infiltration was modestly but significantly (p<0.05) enhanced by aminophylline treatment (Figure 6A–B), while T-cell populations in the spleen were unaffected (Figure 6C). Importantly, AMO treatment enhanced the antitumor efficacy of adoptively-transferred pmel (tumor-specific) T cells into mice with advanced (day 15–18) tumors, as assessed by the level of *trp1* gene expression in lungs, whereas adoptive transfer of pmel T cells into mice without AMO had no significant effect on tumor burden (Figure 6D). Collectively, these data suggest that suppression of chemokine in tumor-bearing lungs is partially due to adenosine accumulation, and that chemotactic activity may be maintained or restored through the use of specific adenosine receptor antagonists.

Our prior data suggest that melanoma is a source of CXCR3-cognate chemokine in the TME, so we assessed the possibility that adenosine suppresses tumor production of chemokine. We confirmed that B16 melanoma expresses the adenosine receptor A_{2A}R (ADORA2A, Figure 7A) as well as *ADORA2A* and *ADORA2B* (which encodes A_{2B}R) gene products (data not shown). *In vitro*, exogenous adenosine suppressed B16 production of CXCL10, even after activation of chemokine production via treatment with IFN γ (Figure 7B). Importantly, the A₂R-specific inhibitor ZM-241,385 (24) significantly reversed adenosine-mediated suppression of CXCL10 (Figure 7B). Similarly, 5 of 7 human melanoma cells lines tested expressed surface A_{2A}R (representative data for line VMM12, Figure 7C), and exogenous adenosine suppressed chemokine production by VMM12 melanoma (Figure 7D).

While the source of adenosine in the TME remains to be determined, we observed an increase in the proportion of regulatory (Foxp3⁺CD4⁺) cells in the day 18 TME (Supplemental Figure 10), and these cells expressed high levels of the ecto-5'-nucleotidase CD73, which converts AMP to adenosine. Thus, infiltrating regulatory cells may mediate the accumulation of bioactive adenosine in the melanoma microenvironment, and this possibility remains under study. Collectively, these data demonstrate that adenosine can suppress, and adenosine receptor antagonism can restore, chemokine production in IFN-stimulated melanoma cells.

Discussion

The failure of immunogenic vaccines to mediate regression of established tumors or metastases has generally been ascribed to an immunosuppressive TME, which arises as a consequence of tumor-derived immunomodulatory factors and the function of suppressor cells. Conversely, vaccines in the adjuvant setting have demonstrated modest clinical effects, suggesting that newly forming metastases may be more susceptible to T-cell infiltration and eradication. Previous literature has not considered the possibility that regulation of cytokine and chemokine in the metastatic TME may be differentially regulated over the course of tumor growth. In a melanoma metastases model, we demonstrated a significant tumor-induced production of CXCR3-cognate chemotactic molecules in the microenvironment, but not in systemic circulation. In animals with substantial tumor burden, chemokine production was suppressed. Thus, our data demonstrate that tumors have a temporal “window of vulnerability” of chemokine production and associated T-cell infiltration.

In keeping with our previous observation that CXCR3-expressing T cells are associated with enhanced survival (10), we found that CXCR3 is essential for T-cell infiltration of lungs bearing early metastatic lesions. The requirement for CXCR3 expression by CD8 T cells to efficiently infiltrate lungs bearing metastatic tumors, while not previously demonstrated, is consistent with the observed association between CXCR3 and T cell access of lungs in situations of viral infection (25,26), graft rejection (27), chronic inflammation (16,28), and non-allergic asthma (29). Our data establish the requirement for CXCR3 expression by CD8 T cells to efficiently infiltrate melanoma-engrafted lungs.

As vaccination with peptide and adjuvant can induce CXCR3-expressing tumor-specific T cells (30), these data suggest the protective aspects of adjuvant setting vaccine may arise from pre-existing tumor-reactive CXCR3⁺CD8⁺ T cells that rapidly infiltrate and eradicate newly-arising tumors, whereas established tumors may be recalcitrant to infiltration by the same cells. By extension, these data suggest that tumors may be conditioned for enhanced T-cell infiltration through pharmacologic or immunologic interventions to restore chemokine production in the local microenvironment, thereby enhancing or inducing the antitumor efficacy of therapeutic-setting vaccines. For example, bacteria have been used to induce CXCL9 and CXCL10 in the TME; recent studies have demonstrated the induction of CXCR3 chemokines in solid melanomas following infection with *Toxoplasma gondii* (31) and in lung metastases following infection with *Trichinella spiralis* (32).

The rapid expression, then contraction, of IFN γ , CXCL9, and CXCL10 in lungs has been observed in an infection model using chronic *Rickettsia conorii* infection (33), suggesting the induction of these factors may be a common response of the reparatory microenvironment to tissue damage. Our data extend this paradigm to cancer, demonstrating that metastatic-like lesions in the lungs rapidly induce IFN γ and chemokine production. The molecular mechanisms of tumor-induced cytokine and chemokine remains under investigation, although we demonstrate that melanoma may be a major contributor of CXCL9 and CXCL10, in keeping with our *in vitro* observation in human melanoma cell lines (9). Surprisingly, a significant number of IFN γ - and chemokine-producing CD4 T

cells, but not NK cells, are apparent in early melanoma-infiltrated lungs. The role of these CD4 cells, and the mechanism by which they infiltrate the lungs, remains under investigation.

The observation that melanoma suppresses interferons, CXCL9, and CXCL10 over the course of metastatic tumor growth has not been reported, and these data have implications for T cell-mediated therapy of cancer. To explain the active suppression of IFNs and chemokines, as opposed to a failure to induce these factors, we assessed the activity of the adenosine signaling axis in this model. Present in both intra- and extra-cellular compartments, in the nanomolar range (34), adenosine suppresses antitumor immune responses and can enhance tumor outgrowth. Cekic and colleagues demonstrated that antagonism of adenosine slows the progression of bladder or breast carcinoma growing as solid tumors in a CXCR3-dependent manner (15); therefore, we evaluated the possibility that adenosine signaling blockade, in the context of metastatic melanoma in the lung, may influence the CXCR3 chemotactic axis. We demonstrate that interfering with adenosine signaling restores IFN γ , CXCL9, and CXCL10 levels and partially reconstitutes T-cell infiltration *in situ*. CD4 cells are significant sources of IFN γ in our model, and adenosine has been shown to suppress IFN γ production in CD4 cells (35). Further, we found that adenosine restores IFN γ -induced production of chemokines by melanoma. Therefore, we conjecture that hypoxia in the microenvironment of advanced metastatic disease leads to an accumulation of adenosine, which suppresses IFN γ and CXCR3-cognate chemokine production, and we are currently validating these mechanisms. Interestingly, the capacity of adenosine to directly suppress CXCL10 production in IFN γ -stimulated melanoma cells indicates a specific blockade of gene expression, suggesting that adenosine-mediated suppression of chemokine in the TME may occur even in the presence of exogenous IFNs. Our data also demonstrate that adenosine receptor-mediated suppression of CXCR3-cognate chemokine extends to human melanoma cells, consistent with the single prior report of A_{2A}R in a single human melanoma cell line (36). Our data demonstrate that blocking adenosine A₂ receptor function is sufficient to restore chemotactic gradients, and our ongoing studies will elaborate the relative contributions of A_{2A}R and A_{2B}R.

A recent study has demonstrated that cutaneous melanomas decrease CXCL9 production as a consequence of immune editing and selection of CXCL9-deficient clones (37). We have not excluded the possibility of immune editing in the metastatic-like model; however, the maintenance of *Ifn γ* , *Cxcl9*, and *Cxcl10* expression in late-stage metastases following aminophylline treatment argues against the selection and predominance of loss-of-function clones in our model.

The paucity of responses to immunogenic vaccines and adoptive transfer protocols suggests the need for adjuvant therapy to induce or restore T-cell infiltration into tumor compartments. While chemokine expression is not sufficient to induce or restore antitumor function, they are essential for effective T-cell chemoattraction and therefore an important aspect of cancer immunotherapy. Collectively, our data demonstrate that CXCR3-cognate ligand expression is required for efficient T cell access of tumor-infiltrated lungs, but these ligands are expressed in a temporally restricted pattern. We further demonstrate a means to partially overcome tumor-induced suppression of lymphocyte chemotaxis, suggesting that

metastases may be conditioned for enhanced or restored chemokine expression and T-cell infiltration, thereby potentially enhancing the therapeutic efficacy of immunogenic but clinically ineffective vaccine platforms.

Supplementary Material

Refer to Web version on PubMed Central for supplementary material.

Acknowledgments

Lenora D. Nunnley provided technical support for some studies. We thank John DeLong and Dr. Jacqueline Channon-Smith (*DartLab*, the Geisel School of Medicine's Immune Monitoring and Cytometry Core Facility) for expert assistance with flow cytometry studies, and Jennifer Fields and Dr. Steven N. Fiering (Dartmouth Transgenic and Genetic Construct Shared Resource) for expert assistance with mouse models. Maryann Mikucki and Dr. Sharon Evans (Department of Immunology, Roswell Park Cancer Institute) provided insightful comments and suggestions.

Support for these studies was provided, in part, by the Geisel School of Medicine at Dartmouth's Immunology Training Grant (USPHS T32 AI007363 to Dr. Charles L. Sentman, sub-award ECT); the Dartmouth Center for Molecular, Cellular, and Translational Immunology (USPHS P30 GM103415 to Dr. William R. Green, sub-award to DWM); the Joanna M. Nicolay Melanoma Research Foundation (Research Scholar Award, ECT); the Melanoma Research Alliance (Young Investigator Award, DWM); and the USPHS (R01 AI089805, YHH; and R01 CA134799, DWM).

Abbreviations

CCR	chemokine receptor
IFN	interferon
ADO	adenosine
PFA	paraformaldehyde

References

1. Slingluff CL, Petroni GR, Yamshchikov GV, Barnd DL, Eastham S, Galavotti H, et al. Clinical and immunologic results of a randomized phase II trial of vaccination using four melanoma peptides either administered in granulocyte-macrophage colony-stimulating factor in adjuvant or pulsed on dendritic cells. *J Clin Oncol.* 2003; 21:4016–26. [PubMed: 14581425]
2. Rosenberg SA, Yang JC, Restifo NP. Cancer immunotherapy: moving beyond current vaccines. *Nat Med.* 2004; 10:909–15. [PubMed: 15340416]
3. Slingluff CL, Yamshchikov G, Neese P, Galavotti H, Eastham S, Engelhard VH, et al. Phase I trial of a melanoma vaccine with gp100(280–288) peptide and tetanus helper peptide in adjuvant: immunologic and clinical outcomes. *Clin Cancer Res.* 2001; 7:3012–24. [PubMed: 11595689]
4. Rabinovich GA, Gabrilovich D, Sotomayor EM. Immunosuppressive strategies that are mediated by tumor cells. *Annu Rev Immunol.* 2007; 25:267–96. [PubMed: 17134371]
5. Clemente CG, Mihm MC, Bufalino R, Zurrida S, Collini P, Cascinelli N. Prognostic value of tumor infiltrating lymphocytes in the vertical growth phase of primary cutaneous melanoma. *Cancer.* 1996; 77:1303–10. [PubMed: 8608507]
6. Erdag G, Schaefer JT, Smolkin ME, Deacon DH, Shea SM, Dengel LT, et al. Immunotype and immunohistologic characteristics of tumor-infiltrating immune cells are associated with clinical outcome in metastatic melanoma. *Cancer Res.* 2012; 72:1070–80. [PubMed: 22266112]
7. Galon J, Costes A, Sanchez-Cabo F, Kirilovsky A, Mlecnik B, Lagorce-Pagès C, et al. Type, density, and location of immune cells within human colorectal tumors predict clinical outcome. *Science.* 2006; 313:1960–4. [PubMed: 17008531]

8. Harlin H, Meng Y, Peterson AC, Zha Y, Tretiakova M, Slingluff C, et al. Chemokine expression in melanoma metastases associated with CD8+ T-cell recruitment. *Cancer Res.* 2009; 69:3077–85. [PubMed: 19293190]
9. Dengel LT, Norrod AG, Gregory BL, Clancy-Thompson E, Burdick MD, Strieter RM, et al. Interferons induce CXCR3-cognate chemokine production by human metastatic melanoma. *J Immunother.* 2010; 33:965–74. [PubMed: 20948440]
10. Mullins IM, Slingluff CL, Lee JK, Garbee CF, Shu J, Anderson SG, et al. CXC chemokine receptor 3 expression by activated CD8+ T cells is associated with survival in melanoma patients with stage III disease. *Cancer Res.* 2004; 64:7697–701. [PubMed: 15520172]
11. Hsueh EC, Essner R, Foshag LJ, Ollila DW, Gammon G, O'Day SJ, et al. Prolonged survival after complete resection of disseminated melanoma and active immunotherapy with a therapeutic cancer vaccine. *J Clin Oncol.* 2002; 20:4549–54. [PubMed: 12454111]
12. Dankort D, Curley DP, Carlidge Ra, Nelson B, Karnezis AN, Damsky WE, et al. Braf(V600E) cooperates with Pten loss to induce metastatic melanoma. *Nat Genet.* 2009; 41:544–52. [PubMed: 19282848]
13. Steinberg SM, Zhang P, Malik BT, Boni A, Shabaneh TB, Byrne KT, et al. BRAF inhibition alleviates immune suppression in murine autochthonous melanoma. *Cancer Immunol Res.* 2014; 2:1044–50. [PubMed: 25183499]
14. Fisher DT, Chen Q, Skitzki JJ, Muhitch JB, Zhou L, Appenheimer MM, et al. IL-6 trans-signaling licenses mouse and human tumor microvascular gateways for trafficking of cytotoxic T cells. *J Clin Invest.* 2011; 121:3846–59. [PubMed: 21926464]
15. Cekic C, Sag D, Li Y, Theodorescu D, Strieter RM, Linden J. Adenosine A2B receptor blockade slows growth of bladder and breast tumors. *J Immunol.* 2012; 188:198–205. [PubMed: 22116822]
16. Nie L, Xiang R, Zhou W, Lu B, Cheng D, Gao J. Attenuation of acute lung inflammation induced by cigarette smoke in CXCR3 knockout mice. *Respir Res.* 2008; 9:82. [PubMed: 19087279]
17. Medoff BD, Wain JC, Seung E, Jakobek R, Means TK, Ginns LC, et al. CXCR3 and Its Ligands in a Murine Model of Obliterative Bronchiolitis: Regulation and Function. *J Immunol.* 2006; 176:7087–95. [PubMed: 16709871]
18. Groom JR, Luster AD. CXCR3 ligands: redundant, collaborative and antagonistic functions. *Immunol Cell Biol.* 2011; 89:207–15. [PubMed: 21221121]
19. Thapa M, Carr DJJ. CXCR3 deficiency increases susceptibility to genital herpes simplex virus type 2 infection: Uncoupling of CD8+ T-cell effector function but not migration. *J Virol.* 2009; 83:9486–501. [PubMed: 19587047]
20. Groom JR, Luster AD. CXCR3 in T cell function. *Exp Cell Res.* 2011; 317:620–31. [PubMed: 21376175]
21. Stagg J, Smyth MJ. Extracellular adenosine triphosphate and adenosine in cancer. *Oncogene.* 2010; 29:5346–58. [PubMed: 20661219]
22. Wallace KL, Marshall Ma, Ramos SI, Lannigan Ja, Field JJ, Strieter RM, et al. NKT cells mediate pulmonary inflammation and dysfunction in murine sickle cell disease through production of IFN-gamma and CXCR3 chemokines. *Blood.* 2009; 114:667–76. [PubMed: 19433855]
23. Hochwald C, Kennedy K, Chang J, Moya F. A randomized, controlled, double-blind trial comparing two loading doses of aminophylline. *J Perinatol.* 2002; 134:275–8. [PubMed: 12032788]
24. Poucher SM, Keddie JR, Singh P, Stoggall SM, Caulkett PW, Jones G, et al. The in vitro pharmacology of ZM 241385, a potent, non-xanthine A2a selective adenosine receptor antagonist. *Br J Pharmacol.* 1995; 115:1096–102. [PubMed: 7582508]
25. Kohlmeier JE, Cookenham T, Miller SC, Roberts AD, Christensen JP, Thomsen AR, et al. CXCR3 directs antigen-specific effector CD4+ T cell migration to the lung during parainfluenza virus infection. *J Immunol.* 2009; 183:4378–84. [PubMed: 19734208]
26. Lindell DM, Lane TE, Lukacs NW. CXCL10/CXCR3-mediated responses promote immunity to respiratory syncytial virus infection by augmenting dendritic cell and CD8(+) T cell efficacy. *Eur J Immunol.* 2008; 38:2168–79. [PubMed: 18624292]

27. Seung E, Cho JL, Sparwasser T, Medoff BD, Luster AD. Inhibiting CXCR3-dependent CD8+ T cell trafficking enhances tolerance induction in a mouse model of lung rejection. *J Immunol.* 2011; 186:6830–8. [PubMed: 2155535]
28. Lin Y, Yan H, Xiao Y, Piao H, Xiang R, Jiang L, et al. Attenuation of antigen-induced airway hyperresponsiveness and inflammation in CXCR3 knockout mice. *Respir Res.* 2011; 12:123. [PubMed: 21939519]
29. Barbarroja-Escudero J, Prieto-Martin A, Monserrat-Sanz J, Reyes-Martin E, Diaz-Martin D, Antolin-Amerigo D, et al. Abnormal chemokine receptor profile on circulating T lymphocytes from nonallergic asthma patients. *Int Arch Allergy Immunol.* 2014; 164:228–36. [PubMed: 25178112]
30. Clancy-Thompson E, King LK, Nunnley LD, Mullins IM, Slingluff CL, Mullins DW. Peptide vaccination in Montanide adjuvant induces and GM-CSF increases CXCR3 and Cutaneous Lymphocyte Antigen expression by tumor antigen-specific CD8 T cells. *Cancer Immunol Res.* 2013; 1:332–9. [PubMed: 24377099]
31. Baird JR, Byrne KT, Lizotte PH, Toraya-Brown S, Scarlett UK, Alexander MP, et al. Immune-Mediated Regression of Established B16F10 Melanoma by Intratumoral Injection of Attenuated *Toxoplasma gondii* Protects against Rechallenge. *J Immunol.* 2013; 190:469–78. [PubMed: 23225891]
32. Kang Y-J, Jo J-O, Cho M-K, Yu H-S, Leem S-H, Song KS, et al. *Trichinella spiralis* infection reduces tumor growth and metastasis of B16-F10 melanoma cells. *Vet Parasitol.* 2013; 196:106–13. [PubMed: 23499484]
33. Valbuena G, Bradford W, Walker DH. Expression analysis of the T-cell-targeting chemokines CXCL9 and CXCL10 in mice and humans with endothelial infections caused by rickettsiae of the spotted fever group. *Am J Pathol.* 2003; 163:1357–69. [PubMed: 14507644]
34. Fredholm BB. Adenosine, an endogenous distress signal, modulates tissue damage and repair. *Cell Death Differ.* 2007; 14:1315–23. [PubMed: 17396131]
35. Erdmann AA, Gao Z-G, Jung U, Foley J, Borenstein T, Jacobson Ka, et al. Activation of Th1 and Tc1 cell adenosine A2A receptors directly inhibits IL-2 secretion in vitro and IL-2-driven expansion in vivo. *Blood.* 2005; 105:4707–14. [PubMed: 15746085]
36. Merighi S, Mirandola P, Milani D, Varani K, Gessi S, Klotz K-N, et al. Adenosine receptors as mediators of both cell proliferation and cell death of cultured human melanoma cells. *J Invest Dermatol.* 2002; 119:923–33. [PubMed: 12406340]
37. Petro M, Kish D, Guryanova Oa, Ilyinskaya G, Kondratova A, Fairchild RL, et al. Cutaneous Tumors Cease CXCL9/Mig Production as a Result of IFN- γ -Mediated Immunoediting. *J Immunol.* 2013; 190:832–41. [PubMed: 23241877]

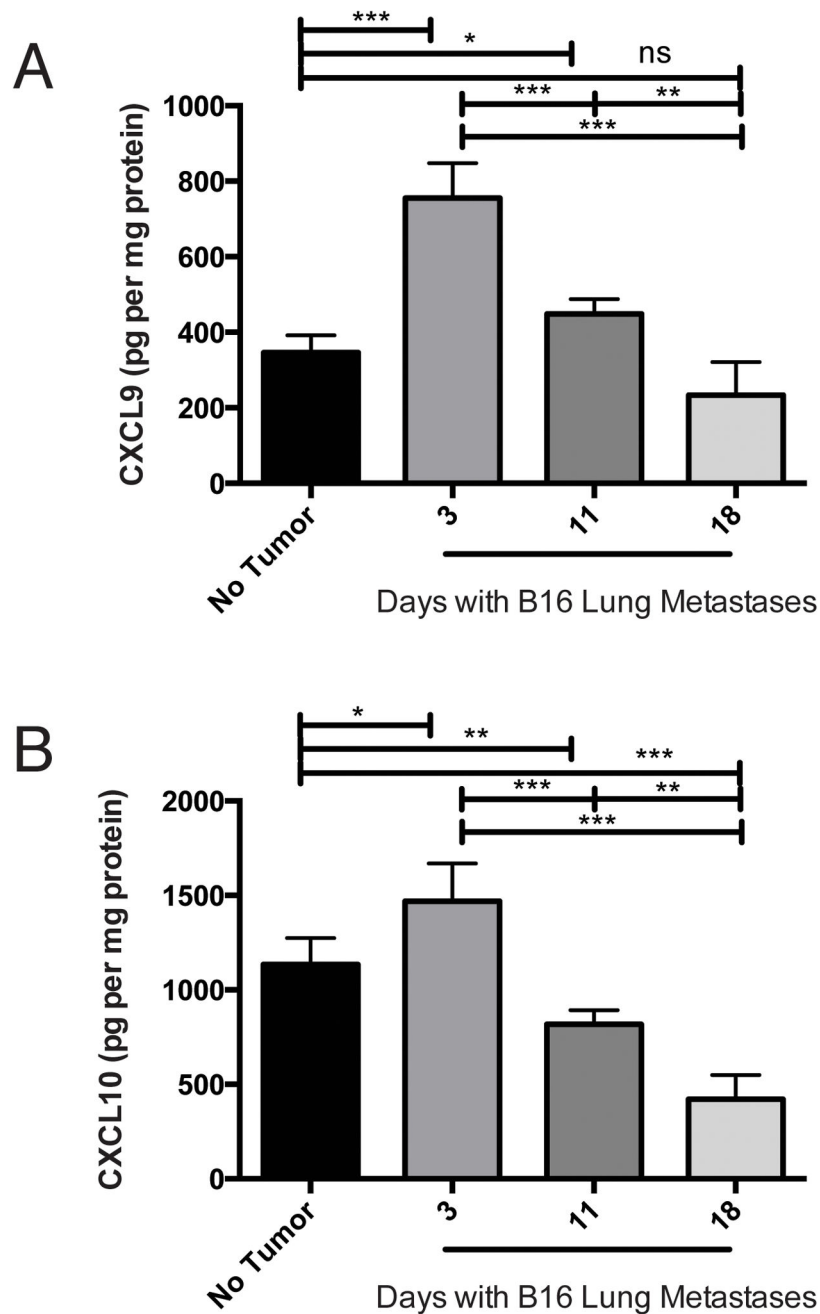


Figure 1. CXCR3-cogate chemokine production is temporally regulated in melanoma-bearing lungs

Mice were given intravenous B16 injection on day 0. At the time points indicated, mice were sacrificed and lungs assessed for A) CXCL9 protein and B) CXCL10 protein.

Expression of *Cxcl9* and *Cxcl10* correlated with observed protein profiles (data not shown).

In all panels, differences were assessed by *T* test, as indicated: *, $p < 0.05$; **, $p < 0.01$; ***, $p < 0.001$.

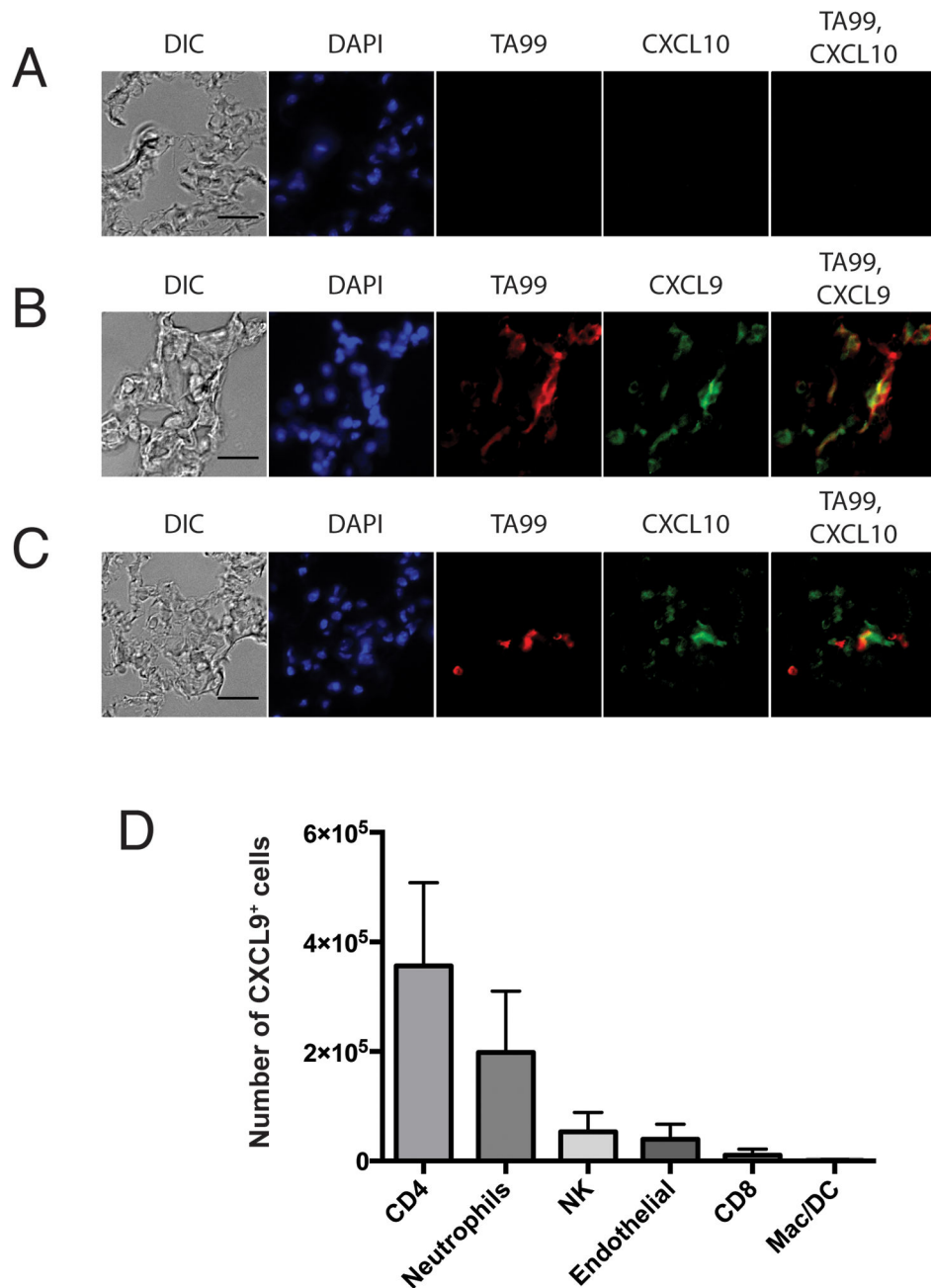


Figure 2. Cellular sources of CXCL9 and CXCL10 in lungs bearing day 3 metastatic-like melanoma

A–C) Light microscopy and immunohistochemical staining for DAPI, melanoma-specific antigen (TA99), and chemokine (CXCL9-10). Lungs from A) tumor free (naïve) mice and B–C) mice intravenously injected 3 days earlier with B16 melanoma were sacrificed and assessed for chemokine production. D) Intracellular flow cytometric evaluation of CXCL9-expressing cells. Lungs from mice with day 3 B16 tumors were processed to single-cell suspensions and stained for intracellular CXCL9 and surface lineage markers.

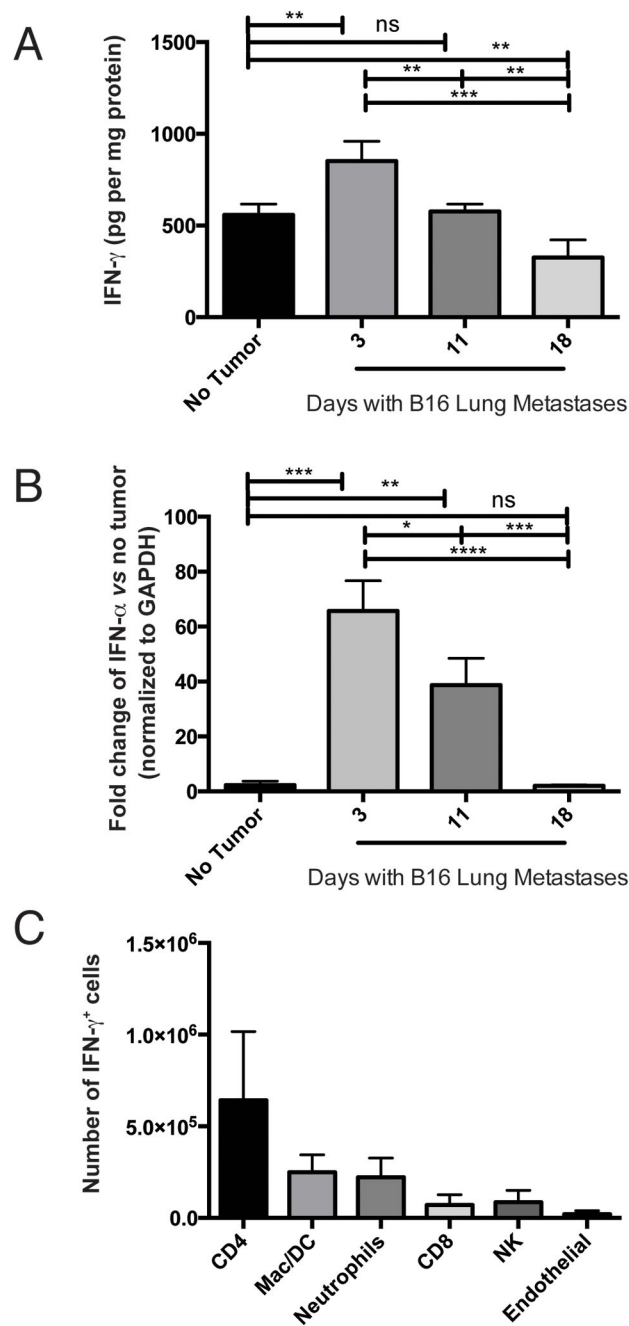


Figure 3. Interferon production is temporally regulated in melanoma-bearing lungs

Mice were given intravenous B16 injection on day 0. At the time points indicated, mice were sacrificed and lungs assessed for A) IFN γ protein and B) *Ifn γ* expression (normalized to GAPDH). Expression of *Ifn γ* correlated with observed protein profiles (data not shown). C) Intracellular flow cytometric evaluation of IFN γ -expressing cells. Lungs from mice with day 3 B16 tumors were processed to single-cell suspensions and stained for intracellular IFN γ and surface lineage markers. In all A–B, differences were assessed by *T* test, as indicated: *, $p < 0.05$; **, $p < 0.01$; ***, $p < 0.001$; ****, $p < 0.0001$.

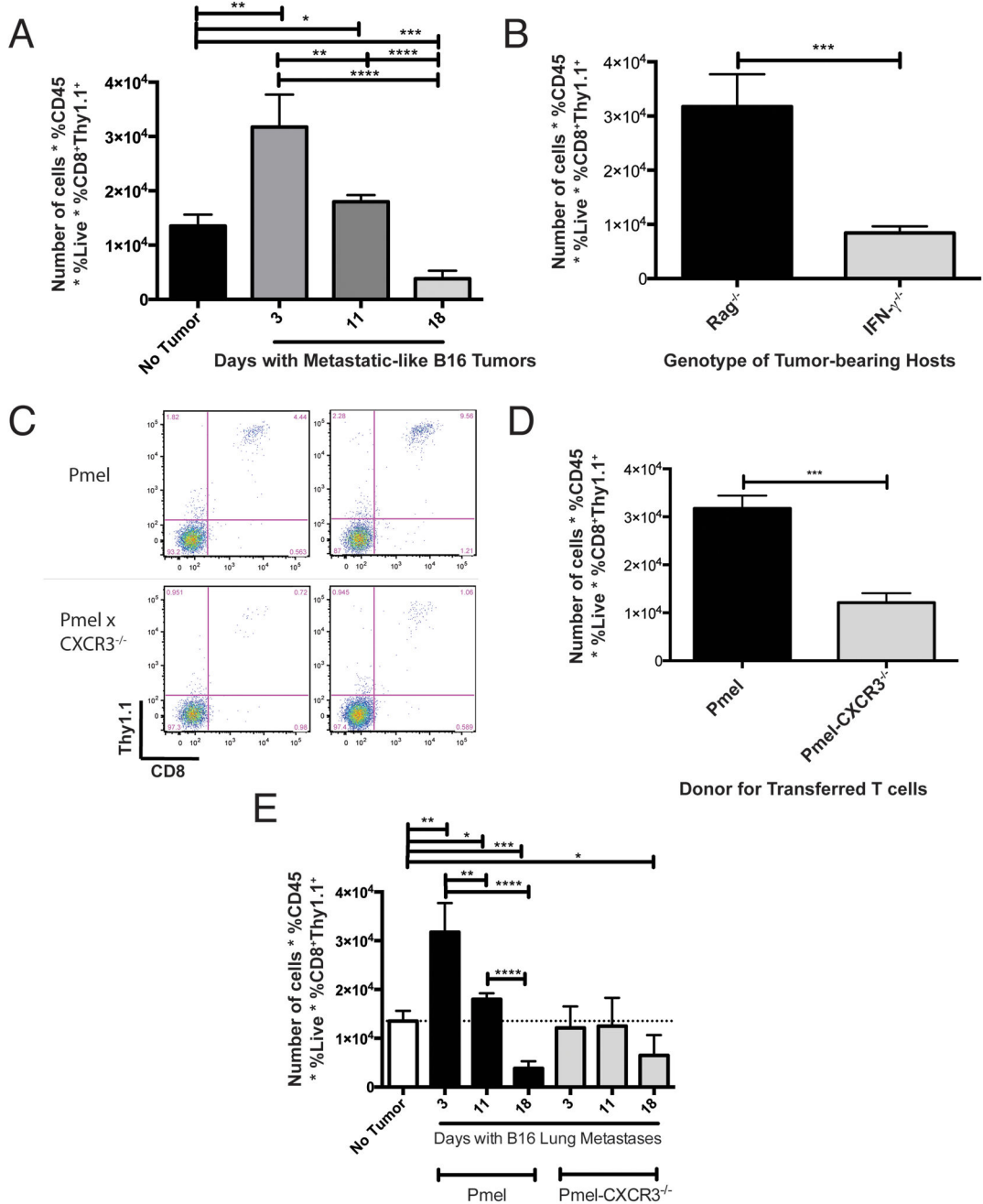


Figure 4. CXCR3-expressing Pmel CD8⁺ T cells traffic to lungs more efficiently than CXCR3-deficient Pmel T cells

To assess T-cell infiltration of tumor-bearing lungs, mice were given intravenous B16 injection on day 0, then received adoptive transfer with either CXCR3^{+/+} (Pmel) or CXCR3^{-/-} (Pmel/CXCR3^{-/-}) tumor antigen-specific CD8⁺ T cells. A) Number of recovered Pmel CD8⁺ T cells from lungs of RAG^{-/-} hosts at various stages of tumor growth. Comparable results were observed using B6 hosts (data not shown). B) Number of recovered Pmel CD8⁺ T cells from lungs of RAG^{-/-} and IFN γ ^{-/-} hosts at day 3 post-tumor challenge. C) Representative flow cytometry data, gated on live CD45⁺ cells in the

lymphocyte FS/SS gate, from lungs of mice with day 3 tumors, following adoptive transfer of Pmel (CXCR3^{wt}) or Pmel/CXCR3^{-/-} cells. D) Number of recovered Pmel or Pmel/CXCR3^{-/-} CD8⁺ T cells from lungs of mice at day 3 post-tumor challenge. E) Number of recovered Pmel or Pmel/CXCR3^{-/-} CD8⁺ T cells from lungs of mice at various times post-tumor challenge. In all panels, differences were assessed by *T* test, as indicated: *, p<0.05; **, p<0.01; ***, p<0.001; ****, p<0.0001.

Author Manuscript

Author Manuscript

Author Manuscript

Author Manuscript

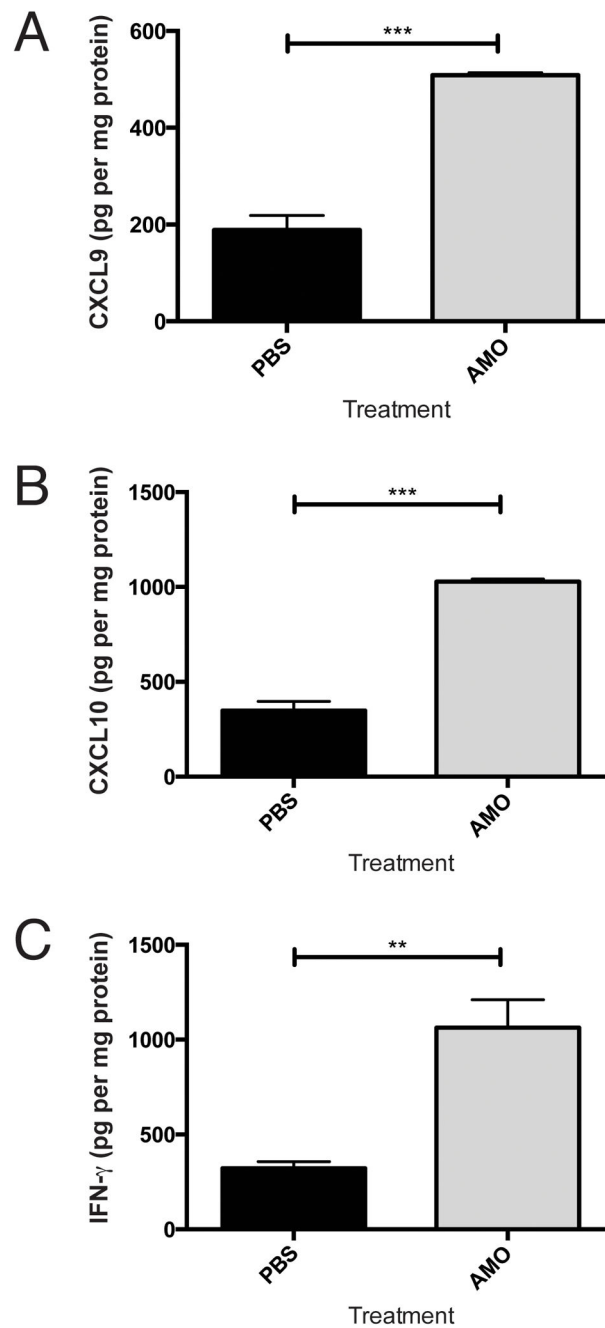


Figure 5. Inflammatory interferon and chemokine levels are increased in aminophylline-treated mice with established lung metastases

Mice were given intravenous B16 injection on day 0. Every 3 days, mice were treated with an I.P. injection of PBS or aminophylline (50mg/kg). On day 18, mice were sacrificed and proteins were harvested from the lungs. A) CXCL9 production. B) CXCL10 production. C) IFN γ production. In all panels, differences were assessed by *T* test: **, $p < 0.01$; ***, $p < 0.001$.

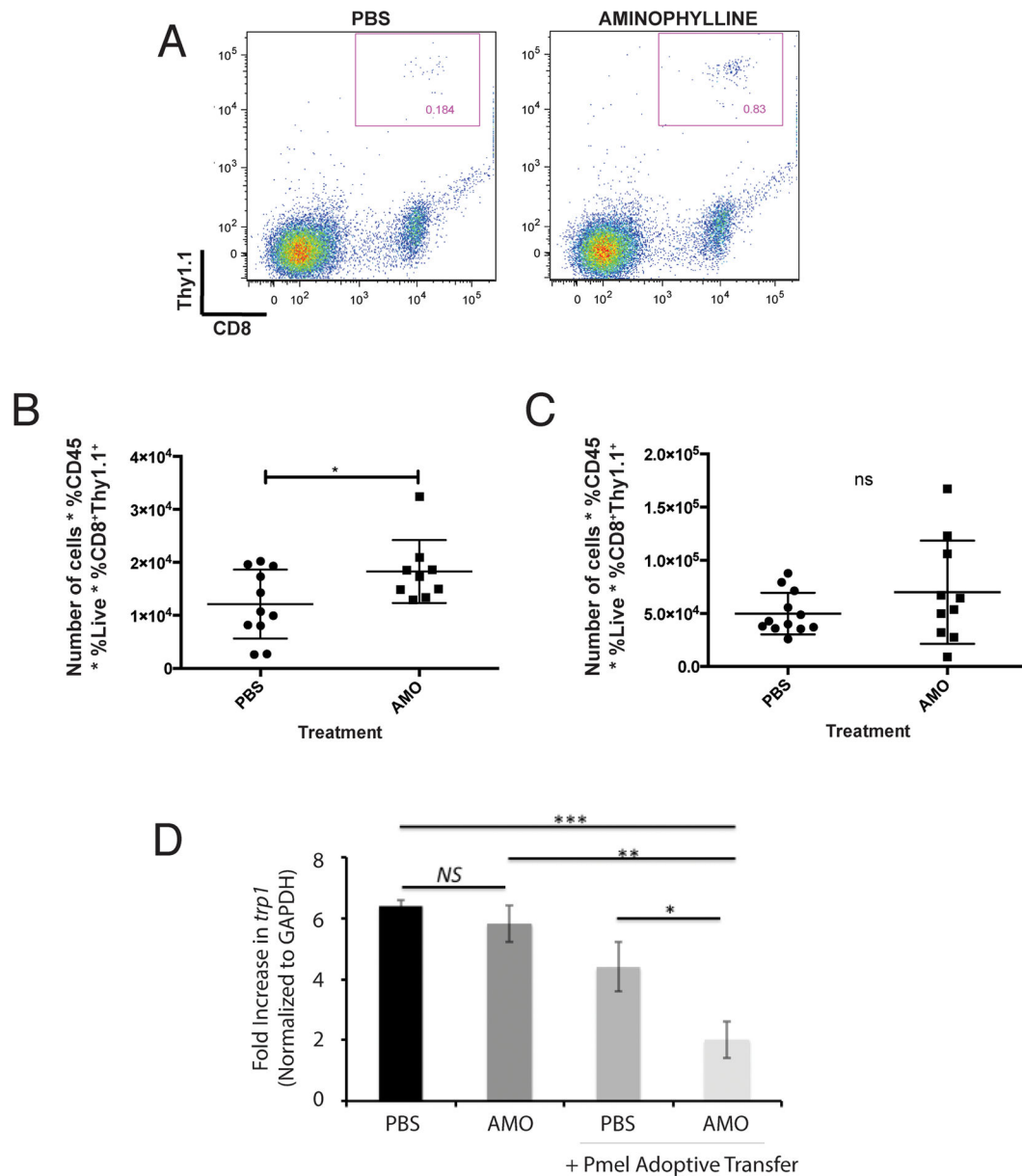


Figure 6. Aminophylline treatment enhances T-cell infiltration of lungs with advanced (day 18) B16 melanoma

Mice were given intravenous B16 injection on day 0. Every 3 days, mice were treated with an I.P. injection of PBS or aminophylline (50mg/kg). Mice received adoptive transfer of 1×10^6 Pmel CD8⁺ T cells on day 18 (for tracking studies A–C) or day 15 (for tumor control study, D). A) Representative flow cytometry of Thy1.1⁺CD8⁺ Pmel T cells in mice treated with PBS or aminophylline. B) Number of recovered Pmel CD8⁺ T cells from lungs of B6 mice treated with PBS or aminophylline. C) Number of recovered Pmel CD8⁺ T cells from spleens of B6 mice treated with PBS or aminophylline. D) Tumor burden in lungs of mice treated with PBS or aminophylline, without or with adoptive transfer (day 15) of Pmel T cells. Assessment of tumor burden at day 18. Differences were assessed by T test: * $p < 0.05$; **, $p < 0.01$; ***, $p < 0.001$.

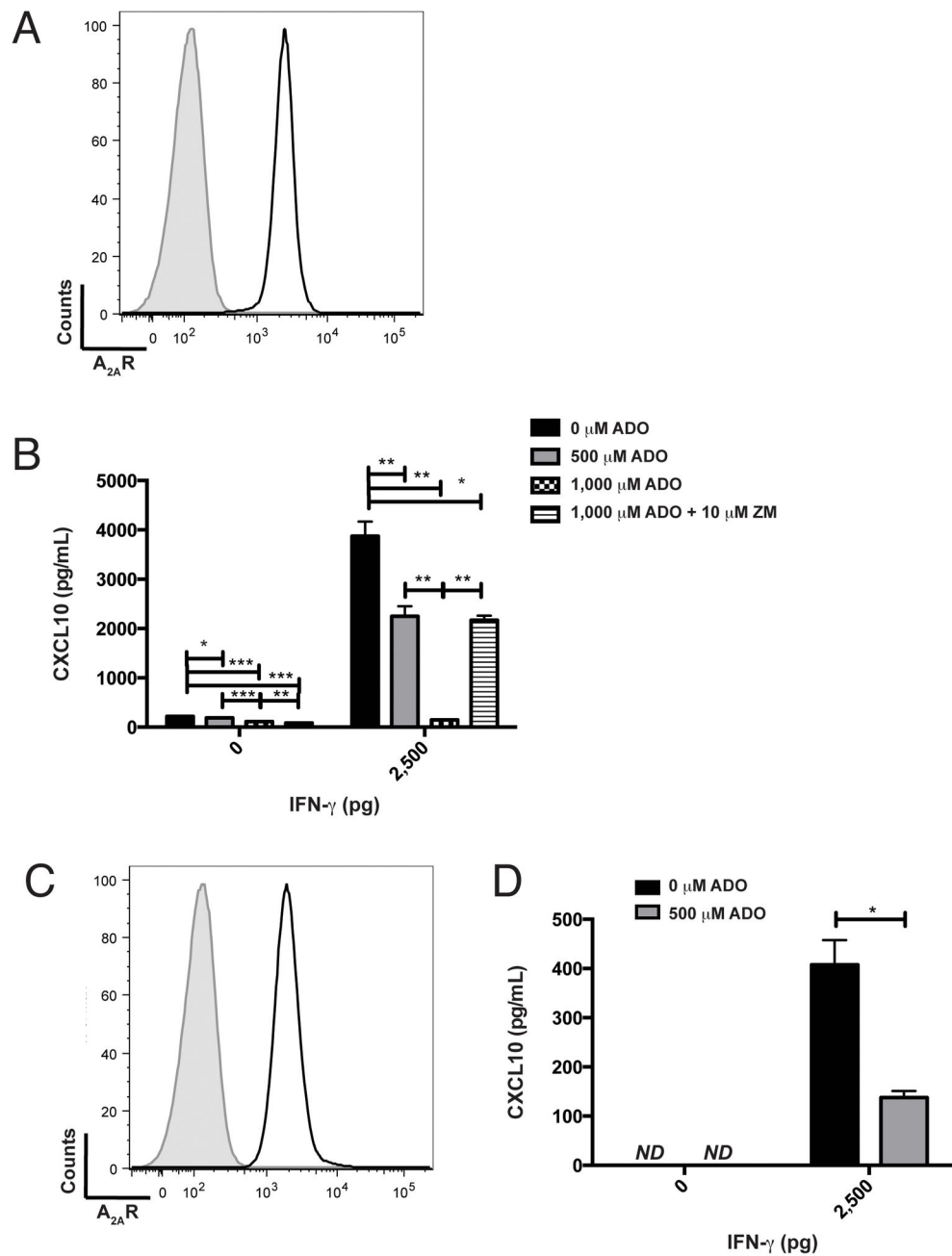


Figure 7. Adenosine suppresses, and adenosine receptor 2 antagonist restores, CXCL10 production by melanoma cells *in vitro*

A) Flow cytometric staining of B16 melanoma for adenosine receptor A_{2A} (ADORA2A). Shaded histogram, unstained; open histogram, $A_{2A}R$ -specific staining. B) Adenosine regulates CXCL10 production by B16 melanoma. Supernatant from B16 melanoma, cultured in the presence or absence of exogenous IFN γ (0pg, 2,500pg), adenosine (ADO) (0 μ M, 500 μ M, 1,000 μ M), and ZM241,385 (ZM) (0 μ M, 10 μ M), was assessed for CXCL10 production by specific ELISA. C) Flow cytometric staining of human VMM12 melanoma for adenosine receptor A_{2A} (ADORA2A). Shaded histogram, unstained; open histogram, $A_{2A}R$ -specific staining. D) Adenosine regulates CXCL10 production by human VMM12

melanoma. Supernatant from VMM12 melanoma, cultured in the presence or absence of exogenous IFN γ (0pg, 2,500pg) and adenosine (0 μ M, 500 μ M) was assessed for CXCL10 production by specific ELISA. Differences were assessed by T test: *p<0.05, **p<0.01, ***p<0.001

Author Manuscript

Author Manuscript

Author Manuscript

Author Manuscript